



Published in final edited form as:

*Angew Chem Int Ed Engl.* 2017 August 07; 56(33): 9825–9828. doi:10.1002/anie.201704773.

## Molecular Magnetic Resonance Imaging of Lung Fibrogenesis with an Oxyamine Based Probe

Dr. Philip A. Waghorn<sup>a</sup>, Chloe M. Jones<sup>a</sup>, Nicholas J. Rotile<sup>a</sup>, Dr. Steffi K. Koerner<sup>a</sup>, Dr. Diego S. Ferreira<sup>a</sup>, Dr. Howard H. Chen<sup>a</sup>, Clemens K. Probst<sup>b</sup>, Prof. Dr. Andrew M. Tager<sup>b</sup>, and Prof. Peter Caravan<sup>a</sup>

<sup>a</sup>A. A. Martinos Center for Biomedical Imaging and the Institute for Innovation in Imaging, Massachusetts General Hospital, Harvard Medical School, 149 13th Street, Suite 2301, Charlestown, Massachusetts 02129, United States

<sup>b</sup>Division of Pulmonary and Critical Care Medicine and the Center for Immunology and Inflammatory Diseases, Massachusetts General Hospital and Harvard Medical School, Boston, MA 02114, United States

### Abstract

Fibrogenesis is the active production of extracellular matrix in response to tissue injury. In many chronic diseases persistent fibrogenesis results in the accumulation of scar tissue, which can lead to organ failure and death. However no non-invasive technique exists to assess this key biological process. All tissue fibrogenesis results in the formation of allysine, which enables collagen cross-linking and leads to tissue stiffening and scar formation. We report here a novel allysine-binding gadolinium chelate (GdOA), that can non-invasively detect and quantify the extent of fibrogenesis using magnetic resonance imaging (MRI). We demonstrate that GdOA signal enhancement correlates with extent of disease and is sensitive to therapeutic response.

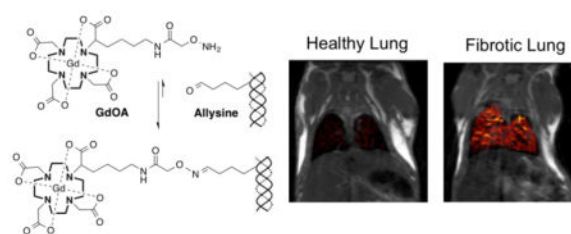
### Graphical Abstract

A key biochemical feature of fibrogenesis is the oxidation of lysine residues on collagen to give allysine, which is responsible for collagen cross-linking, fibril formation, and scar tissue deposition in fibrotic diseases. The oxyamine functionalized molecular probe GdOA binds to allysine leading to MRI signal enhancement in a fibrotic lung disease model, providing a quantitative readout of fibrogenesis.

---

Correspondence to: Peter Caravan.

Electronic Supplementary Information (ESI) for this article is given via a link at the end of the document, containing detailed experimental procedures for compound syntheses, relaxivity measurements, binding and stability study measurements, animal model and MR protocols, full methods for analytical assays and full imaging and assay analysis.



## Keywords

fibrosis; aldehydes; Imaging agents; allysine; collagen

Almost half of deaths in the industrialized world can be attributed to diseases with a fibroproliferative component.<sup>[1]</sup> In the lung, pulmonary fibrosis constitutes a major cause of morbidity and mortality. Idiopathic pulmonary fibrosis (IPF), the most common and most lethal diffuse fibrosing lung disease, is responsible for an estimated 40,000 deaths per year in the US.<sup>[2]</sup> Pulmonary fibrosis is characterized by the accumulation of myofibroblasts and their production of an excess of extracellular matrix (ECM) proteins. Though this ECM accumulation and remodeling, termed fibrogenesis, is an innate part of the natural wound healing process, under persistent injury excess ECM results in a build up of scar tissue causing loss of tissue function and potential organ failure and mortality.<sup>[3]</sup>

High-resolution computed tomography is invaluable for the diagnosis of IPF,<sup>[4]</sup> but cannot distinguish regions of active fibrogenesis from stable scar. Molecular MRI, to quantify the extent of increased ECM components, by direct targeting of the collagen deposition that occurs during scar tissue formation, has previously been used to image fibrosis.<sup>[5]</sup> While this provides a means to quantify the changes in total fibrotic burden of a patient, collagen imaging does not provide a measure of the dynamic changes occurring at the molecular level during fibrogenesis. Imaging fibrogenesis would identify patients whose disease is progressing and would also enable monitoring of treatment with drugs that could stop or slow fibrotic progression.

A universal feature of fibrogenesis is the oxidation of ECM lysine residues, chiefly in collagen, to the aldehyde allysine by the lysyl-oxidase (LOX) family of enzymes. Allysine<sup>[6]</sup> undergoes a series of condensation reactions with other amino acids on neighboring collagen molecules (Fig. S1) to form irreversible cross-links that stabilize the ECM, and is a fundamental feature across all fibrotic diseases.<sup>[7]</sup> While lysine oxidation is catalyzed by LOX, the subsequent condensation reactions of allysine are slower. We reasoned that allysine could be a target for imaging fibrogenesis. In active fibrogenesis an increased pool of allysine would be generated, but in stable disease or with therapeutic intervention these allysine moieties would be converted to crosslinks.

To determine if allysine was sufficiently abundant for detection with MRI we quantified allysine in mouse lung tissue using HPLC. Normal and fibrotic lung tissue was digested at 110 °C in 6 M HCl for 24 h, and the allysine derivatized with 2-naphthol-7-sulfonate to yield a fluorescent molecule that could be detected and quantified by HPLC.<sup>[8]</sup> In normal

mouse lung, there was  $80 \pm 6$  nmol allysine per gram of lung tissue,  $\sim 80 \mu\text{M}$ . In mice injured with bleomycin, the allysine concentration content was increased to  $150 \pm 16$  nmol/g. Such high micromolar concentrations are readily detectable by Gd-enhanced MRI.

In the design of a probe for MR imaging of fibrogenesis, certain criteria are essential. These include: i) high thermodynamic and kinetic chelate stability, ii) high water solubility, iii) rapid renal excretion, iv) low non-target background uptake, v) rapid penetration into the tissue interstitial space, and vi) target selectivity. To satisfy these criteria we developed GdOA, an oxyamine-functionalized derivative of GdDOTA for targeting allysine. The GdDOTA core provides a highly stable and inert Gd-chelate (Fig S2). The anionic and hydrophilic nature of GdOA results in high solubility, reduces nonspecific protein binding, and promotes rapid renal elimination. For target selectivity an oxyamine was selected, as the oxime formed from the reaction of an aldehyde with an oxyamine is known to be more stable to hydrolysis than their analogous hydrazone or imine,<sup>[9]</sup> and therefore expected to result in a strong MR signal enhancement on binding to allysine.

GdOA (Fig. 1a, SI Scheme 1) was prepared by coupling the NHS active-ester of *N*-Boc-aminoxyacetic acid<sup>[10]</sup> with an amine-functionalized derivative of DOTA (DOTA-NH<sub>2</sub>), followed by Boc-deprotection in 1 M HCl, with subsequent Gd chelation at pH 6.8. GdOA purity was assessed by HPLC-ICP-MS analysis, with a single Gd species identified and confirmed as GdOA by HPLC-MS analysis. A six-carbon chain was used as a linker to minimize interaction between the GdDOTA core and oxyamine. As a negative control, GdOX was synthesized which has the same pharmacokinetic properties of GdOA, but is incapable of undergoing a condensation reaction with allysine (Fig. 1a, SI Scheme 2).

The relaxivity (1.4 T, 37 °C) of GdOA was similar when measured in PBS solution ( $4.25 \text{ mM}^{-1}\text{s}^{-1}$ ) or in PBS with 3 mg bovine serum albumin (BSA,  $150 \mu\text{M}$ ) indicating very low nonspecific protein binding. However in the presence of 3 mg BSA that had been oxidized with FeCl<sub>3</sub>/aspartate to generate 16 nmol of aldehydes per mg of protein,<sup>[11]</sup> relaxivity increased by 90% to  $8.10 \text{ mM}^{-1}\text{s}^{-1}$  (Fig. 1b); the protein-bound fraction of GdOA had a relaxivity of  $16.87 \text{ mM}^{-1}\text{s}^{-1}$ . GdOX showed negligible increase in relaxivity in the presence of BSA or oxidized BSA-Ald. Quantification of GdOA probe bound to BSA-Ald, following ultrafiltration and ICP-MS analysis, gave a binding constant of  $164 \mu\text{M}$  (Fig. 1c). To assess inertness, GdOA was challenged with zinc and phosphate and showed no Gd release (Fig. S2).

Next the binding of GdOA to tissue was assessed. Aorta is rich in allysine as a result of high lysyl-oxidase activity and turnover of elastin and collagen. We measured  $7.50 \mu\text{mol}$  of allysine per gram of porcine aorta using the HPLC assay. We then incubated GdOA or GdOX with segments of aorta (25 mg aorta, 37 °C, 24 h, pH 7). After repeat washing to remove non-specifically bound probe, the aorta associated Gd was quantified by ICP-MS analysis. GdOA gave a  $K_d$  of  $360 \mu\text{M}$ , while GdOX showed no affinity (Fig. 1d).

The pharmacokinetics of GdOA and GdOX were assessed in naive mice using MR imaging to measure the blood MR signal wash-out from the left ventricle of the heart. Both probes displayed rapid and almost identical blood clearances with blood half-lives of 5.5 and 6.1

minutes for GdOA and GdOX respectively, indicating comparable probe pharmacokinetics (Fig. S3). Elimination was exclusively through the kidneys with minimal, transient liver enhancement observed. Biodistribution of Gd-OA at 1 hour after bolus intravenous injection in naïve C57Bl/6 mice showed that 95% of the injected dose had already been eliminated from the body (Table S1).

The ability of GdOA to detect and stage pulmonary fibrogenesis was then evaluated using a bleomycin lung injury mouse model. Bleomycin is a chemotherapeutic antibiotic,<sup>[12]</sup> but a major adverse effect of bleomycin is the overproduction of reactive oxygen species in the lung,<sup>[13]</sup> which can lead to fibrosis.<sup>[14]</sup> Mice injured with bleomycin rapidly and reliably develop pulmonary fibrosis.<sup>[15]</sup> We studied four groups of mice: Group 1) mice injured with a single intratracheal administration of bleomycin (Bleo); Group 2) age-matched healthy mice (Naive); Group 3) mice injured with bleomycin and then dosed daily with the pan-LOX inhibitor  $\beta$ -aminopropionitrile (BAPN, 100 mg/kg) (Bleo+BAPN);<sup>[16]</sup> and Group 4) mice injured with bleomycin and then dosed daily with PBS as a vehicle control (Bleo+PBS). After 14 days, mice were imaged before and after intravenous injection of 100  $\mu$ mol/kg GdOA (all 4 cohorts) or GdOX (first 2 cohorts), the same dose used for most clinical GdDOTA enhanced MRI exams.<sup>[17]</sup>

Bleomycin-injured mice demonstrated increased pulmonary fibrosis as measured by the Ashcroft system of histology scoring (Fig. S4). Bleomycin-injured mice had 3.4-fold higher lung LOX activity (Fig. 2a, Fig. S5), 1.75-fold higher collagen content (Fig. S6), and 2.1-fold higher allysine content (Fig. 2b, Fig. S7) than in naive animals. Treatment with LOX inhibitor BAPN reduced lung LOX activity and allysine content to levels observed in naive mice, although BAPN had no effect on total lung collagen levels (Fig. 2a–b).

It is well known that T2\* in the lung is very short (~1 ms) because of the magnetic susceptibility gradients caused by the air-tissue interface. In order to overcome this signal loss we used an ultrashort echo time (UTE) sequence. T1-weighted UTE MR images were taken before and after injection of GdOA or GdOX (Fig. 2c,d,g, Fig. S8), starting at 12 minutes when background blood signal was minimal and lung signal intensity was highest. The lung signal and adjacent skeletal muscle signal were measured before and after probe injection, and the change in lung-to-muscle signal ratio ( LMR) (Fig. 2e, Fig. S9) was calculated, where  $LMR = SI_{lung} / SI_{muscle}$  (SI = signal intensity), and  $LMR = LMR_{post} - LMR_{pre}$ . GdOA injection resulted in strong lung signal enhancement in bleomycin-injured lungs compared to naive mice. Signal enhancement correlated strongly with the extent of disease (Fig. S10). GdOX injection resulted in similar, weak lung enhancement in both bleomycin and naive mice, indicating that the oxyamine function was required for the higher signal observed in the bleomycin-injured mice. BAPN treatment did not inhibit collagen production (Fig. S6), but did prevent allysine production and crosslinking (Fig. 2b). MRI indicated that GdOA is sensitive to the allysine reduction caused by BAPN, further demonstrating the specificity of GdOA (Fig. 2h). We also compared the change in liver-to-muscle ratio between naive and bleomycin-groups after GdOA and saw no significant difference in signal, suggesting that the increased GdOA lung enhancement observed in bleomycin-mice is disease-dependent (Fig. S11). Ex vivo analysis of lung Gd confirmed the

imaging results, with the micromolar Gd lung concentrations measured consistent with the image enhancement observed (Fig. 2f, Fig. S12).

In summary, we showed that alllysine is a suitable target for molecular MR detection of fibrogenesis. The novel probe GdOA is stable with respect to Gd release, and is able to bind to oxidized collagen present during fibrogenesis. GdOA shows rapid uptake in a disease model of pulmonary fibrosis, and demonstrates specific alllysine targeting resulting in enhanced MRI signal in fibrotic tissue. GdOA shows low nonspecific binding and rapid background clearance. GdOA imaging provides a quantitative non-invasive measure of the extent of active fibrogenesis in fibrotic diseases. Targeting alllysine as a readout of the rate of fibrogenesis will allow for determination of fibrotic disease activity across all tissue types.

## Supplementary Material

Refer to Web version on PubMed Central for supplementary material.

## Acknowledgments

Financial support from the National Institutes of Health grants: EB009062, DK104302, HL116315, HL131907, HL133153, OD010650 and RR023385 is gratefully acknowledged.

## References

1. a) Wynn T. J Pathol. 2008; 214:199–210. [PubMed: 18161745] b) Friedman SL, Sheppard D, Duffield JS, Violette S. Science Transl Med. 2013; 5:167sr1.c) Rockey DC, Bell PD, Hill JA. New Engl J Med. 2015; 372:1138–1149. [PubMed: 25785971]
2. a) Olson AL, Swigris JJ, Lezotte DC, Norris JM, Wilson CG, Brown KK. Am J Resp Crit Care. 2007; 176:277–284.b) Raghu G, Weycker D, Edelsberg J, Bradford WZ, Oster G. Am J Resp Crit Care. 2006; 174:810–816.
3. Rafii R, Juarez MM, Albertson TE, Chan AL. J Thorac Dis. 2013; 5:48–73. [PubMed: 23372951]
4. Noble PW, Barkauskas CE, Jiang D. J Clin Inv. 2012; 122:2756–2762.
5. a) Caravan P, Das B, Deng Q, Dumas S, Jacques V, Koerner SK, Kolodziej A, Looby RJ, Sun WC, Zhang Z. Chemical Comm. 2009:430–432.b) Caravan P, Das B, Dumas S, Epstein FH, Helm PA, Jacques V, Koerner S, Kolodziej A, Shen L, Sun WC. Angew Chem Int Ed. 2007; 46:8171–8173.c) Caravan P, Yang Y, Zachariah R, Schmitt A, Mino-Kenudson M, Chen HH, Sosnovik DE, Dai G, Fuchs BC, Lanuti M. Am J Resp Cell Mol. 2013; 49:1120–1126.d) Fuchs BC, Wang H, Yang Y, Wei L, Polasek M, Schühle DT, Lauwers GY, Parkar A, Sinskey AJ, Tanabe KK. J Hepatol. 2013; 59:992–998. [PubMed: 23838178] e) Polasek M, Fuchs BC, Uppal R, Schühle DT, Alford JK, Loving GS, Yamada S, Wei L, Lauwers GY, Guimaraes AR. J Hepatol. 2012; 57:549–555. [PubMed: 22634342] f) Farrar CT, DePeralta DK, Day H, Rietz TA, Wei L, Lauwers GY, Keil B, Subramaniam A, Sinskey AJ, Tanabe KK. J Hepatol. 2015; 63:689–696. [PubMed: 26022693]
6. Kagan HM, Li W. J Cell Biochem. 2003; 88:660–672. [PubMed: 12577300]
7. a) Pinnell SR, Martin GR. Proc Nat Acad Sci. 1968; 61:708–716. [PubMed: 5246001] b) Tanzer ML. Science. 1973; 180:561–566. [PubMed: 4573393] c) Siegel RC. Proc Natl Acad Sci. 1974; 71:4826–4830. [PubMed: 4531019] d) Bornstein P, Kang AH, Piez KA. Proc Nat Acad Sc. 1966; 55:417–424. [PubMed: 5220959]
8. Umeda H, Kawamorita K, Suyama K. Amino acids. 2001; 20:187–199. [PubMed: 11332453]
9. Kalia J, Raines RT. Angew Chem. 2008; 120:7633–7636.
10. Foillard S, Rasmussen MO, Razkin J, Boturyn D, Dumy P. J Org Chem. 2008; 73:983–991. [PubMed: 18173281]

11. a) Levine R. *Method Enzymol.* 1990;465–478. b) Levine RL. *J Biol Chem.* 1983; 258:11828–11833. [PubMed: 6137484] c) Chao CC, Ma YS, Stadtman ER. *Proc Natl Acad Sci.* 1997; 94:2969–2974. [PubMed: 9096330]
12. a) Adamson I. *Environmental Health Perspectives.* 1976; 16:119. [PubMed: 65280] b) Umezawa H, Ishizuka M, Maeda K, Takeuchi T. *Cancer.* 1967; 20:891–895. [PubMed: 5337399]
13. Claussen CA, Long EC. *Chem Rev.* 1999; 99:2797–2816. [PubMed: 11749501]
14. Chaudhary NI, Schnapp A, Park JE. *Am J Resp Crit Care.* 2006; 173:769–776.
15. Usuki J, Fukuda Y. *Pathol Int.* 1995; 45:552–564. [PubMed: 7496500]
16. Tang S-S, Trackman P, Kagan H. *J Biol Chem.* 1983; 258:4331–4338. [PubMed: 6131892]
17. Herborn CU, Honold E, Wolf M, Kemper J, Kinner S, Adam G, Barkhausen J. *Invest Radiol.* 2007; 42:58–62. [PubMed: 17213750]

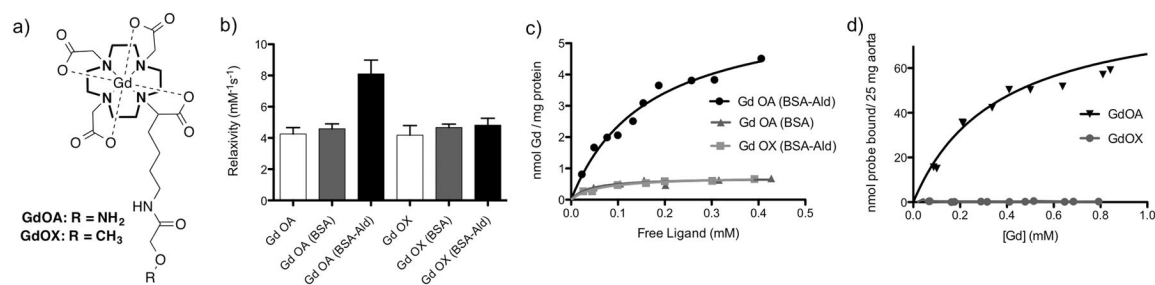


**Figure 1.**

a) Structure of GdOA and GdOX, b) Relaxivity measurements for GdOA, and GdOX incubated in PBS (10 mM, pH 7.4, 37 °C) (white bar), BSA (3 mg protein, PBS, pH 7.4, 37 °C) (grey bar) and with BSA-Ald (3 mg protein, PBS, pH 7.4, 37 °C) (black bar), show a significant increase in relaxivity for GdOA with BSA-Ald indicating probe binding to aldehyde-rich BSA, c) binding curves of GdOA and GdOX incubated with BSA-Ald and BSA, show that GdOA binds to the aldehyde-rich BSA with a  $K_d$  of 164  $\mu$ M (data from  $n=3$ ). d) binding curves of GdOA and GdOX with aorta show that only GdOA binds to alllysine-rich porcine aorta, with  $K_d$  of 360  $\mu$ M (data from  $n=2$ ).



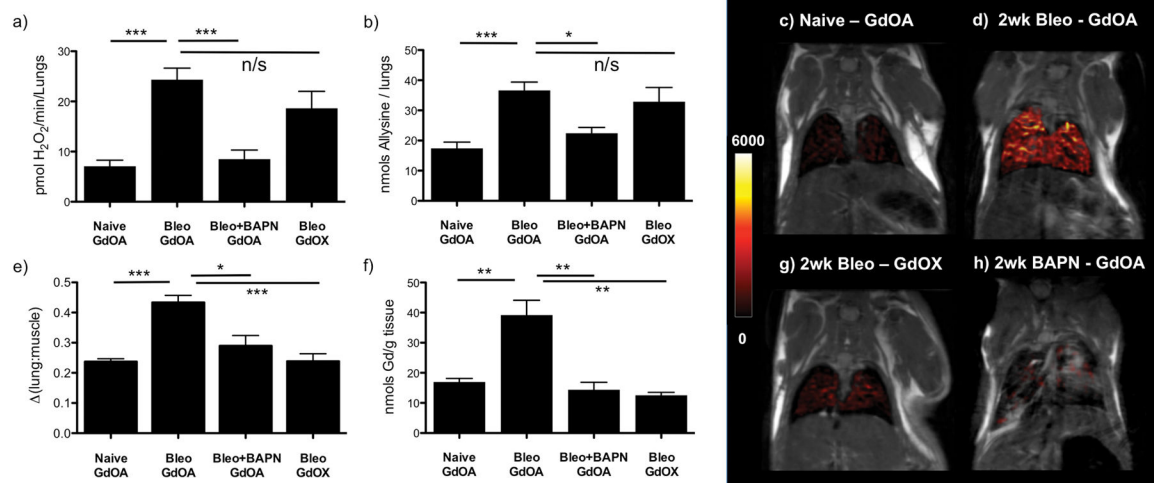


**Figure 2.**

Post imaging ex-vivo tissue analyses for GdOA and GdOX in Naïve, 14 day bleomycin (Bleo) mice, and 14 day bleomycin + daily BAPN (Bleo+BAPN) treated mice and coronal MR images with overlaid lung enhancement (shown in false color): a) total LOX activity levels increased in Bleo treated mice compared to naive animals. Daily BAPN dosing reduces LOX activity levels in Bleo+BAPN animals down to similar levels seen in naive mice, b) allysine lung concentration levels track with LOX activity, with a significant increase in Bleo mice compared to naive animals and a significant decrease in Bleo+BAPN animals, c) GdOA uptake in naive mouse, showing low MR signal enhancement in healthy lungs, d) GdOA uptake in bleomycin-treated mouse, showing strong lung enhancement in 14-day bleomycin-injured mice, e) Image quantification of  $\Delta$  (lung:muscle) ratio, f) Gd concentration in lung tissue, g) GdOX uptake in bleomycin-challenged mouse, showing low lung enhancement in 14-day bleomycin-injured mice with negative control probe and h) GdOA in bleomycin-challenged mouse dosed daily for 14 days with BAPN, showing little lung enhancement, indicating an absence of allysine. (\*:P < 0.05, \*\*: P<0.01, \*\*\*: P< 0.001, n/s: not significant).